

## ***Ab initio* molecular-dynamics study of supercritical carbon dioxide**

Moumita Saharay<sup>a)</sup> and Sundaram Balasubramanian<sup>b)</sup>

*Chemistry and Physics of Materials Unit, Jawaharlal Nehru Centre for Advanced Scientific Research, Jakkur, Bangalore 560 064, India*

(Received 15 December 2003; accepted 18 February 2004)

Car–Parrinello molecular-dynamics simulations of supercritical carbon dioxide (scCO<sub>2</sub>) have been performed at the temperature of 318.15 K and at the density of 0.703 g/cc in order to understand its microscopic structure and dynamics. Atomic pair correlation functions and structure factors have been obtained and good agreement has been found with experiments. In the supercritical state the CO<sub>2</sub> molecule is marginally nonlinear, and thus possesses a dipole moment. Analyses of angle distributions between near neighbor molecules reveal the existence of configurations with pairs of molecules in the distorted T-shaped geometry. The reorientational dynamics of carbon dioxide molecules, investigated through first- and second-order time correlation functions, exhibit time constants of 620 and 268 fs, respectively, in good agreement with nuclear magnetic resonance experiments. The intramolecular vibrations of CO<sub>2</sub> have been examined through an analysis of the velocity autocorrelation function of the atoms. These reveal a red shift in the frequency spectrum relative to that of an isolated molecule, consistent with experiments on scCO<sub>2</sub>. The results have also been compared to classical molecular-dynamics calculations employing an empirical potential.

© 2004 American Institute of Physics. [DOI: 10.1063/1.1701838]

### **I. INTRODUCTION**

The search for nontoxic, recyclable and environmentally benign solvents for use as reaction media, and as cleaning agents is imperative. At least two classes of solvents hold promise in this area—supercritical carbon dioxide (scCO<sub>2</sub>) and room temperature ionic liquids (RTIL).<sup>1–4</sup> Chemical reactivity<sup>5</sup> and catalysis<sup>6,7</sup> in these “green” solvents have been widely studied. scCO<sub>2</sub> in particular, possesses the ability to dissolve fluoropolymers and has been demonstrated to be a substitute for chlorofluorocarbons (CFCs).<sup>8</sup> These studies are being complemented by much research on the microscopic nature of these systems to gain an understanding of the molecular properties.

The structure and dynamics of scCO<sub>2</sub>, its interface with water, and ternary microemulsions of scCO<sub>2</sub>, water and fluorinated surfactants have been studied extensively using experiments<sup>9,10</sup> and by computer simulation methods.<sup>11–13</sup> These simulations employed an empirical interaction model for the constituent molecules which was based on both quantum-chemical calculations as well as from equation of state data. Independent validation of such simulations come from neutron and x-ray diffraction experiments.<sup>14–16</sup> It is crucial that such simulations are also verified by molecular-dynamics calculations that do not depend on empirical potentials. We employ the CPMD approach here in order to understand the microscopic structure and dynamics of *neat* scCO<sub>2</sub>. CPMD calculations are relatively free of empiricism and can thus validate empirical potential models. However, one pays for the increased fidelity in atomic interactions with

a limit in the size of the systems and in the time span that can be studied. Such simulations can also be used to fine tune interaction parameters of empirical potentials<sup>17</sup> which can then be employed to study systems of larger sizes which are more relevant for the supercritical state.<sup>18</sup> More importantly, CPMD simulations can shed light on the molecular structure and solvation dynamics of the solvent and are thus essential in their own right.<sup>19</sup> *This is the primary purpose of our study.*

Our larger aims are to study the solvation of small molecules, including small chain fluoroalkanes, and chemical reactions in scCO<sub>2</sub>, using the *ab initio* MD method. As a first inquiry, we are interested in characterizing the pristine solvent. We present such a study in this article. We compare the results of CPMD to calculations of classical MD that use an empirical potential in order to (i) study system size effects, and (ii) identify differences in the results which could aid one to construct better interaction potentials. In the following, we use the acronym MD to denote molecular-dynamics simulations which used the elementary physical model (EPM2) empirical potential,<sup>20</sup> and CPMD to denote Car–Parrinello molecular-dynamics simulations.

The critical point of CO<sub>2</sub> ( $T_c = 31.1$  °C, and  $P_c = 73.8$  bar) is reasonably close to ambient conditions. Neutron<sup>14,16,21</sup> and x-ray<sup>15</sup> diffraction experiments on scCO<sub>2</sub> have shown significant structural correlations in the first coordination shell. These experiments and MD simulations using empirical potentials have shown the presence of T-shaped near-neighbor configurations of CO<sub>2</sub> molecules in the supercritical state, particularly at high densities.<sup>21</sup> This arrangement is believed to arise out of the nonzero quadrupole moment of the CO<sub>2</sub> molecule and is supposed to compete against a relatively less probable, parallel configuration of nearest neighbors. A proper understanding of the local structure and reorientational dynamics of *neat* CO<sub>2</sub> in the

<sup>a)</sup>Electronic mail: moumita@jncasr.ac.in

<sup>b)</sup>Author to whom correspondence should be addressed. Electronic mail: bala@jncasr.ac.in

supercritical state is thus required in order to understand its ability to solvate a variety of species. With this aim, we report results of *ab initio* MD calculations of scCO<sub>2</sub>. For comparison we have also performed MD calculations using an established empirical potential. Anticipating our results, we observe the CO<sub>2</sub> molecule in the supercritical state to exhibit a marginal nonlinearity in its geometry which will impart it a dipole moment. The supercritical fluid is reasonably well structured, and the time scale of reorientation of a molecule is 620 fs. At the state point calculated here, we observe near neighbor molecules to be present in the distorted T-shaped geometry. In the following section, we describe the details of the calculations performed, followed by a presentation of the results. Conclusions drawn from this work are discussed later.

## II. DETAILS OF SIMULATION

The CPMD and the classical MD calculations were performed at a temperature of 318.15 K and at a density of 0.703 g/cc (or 9.57 molecules nm<sup>-3</sup>), one of the state points studied in Ref. 22. The former were carried out using the CPMD code,<sup>23</sup> for a system of 32 CO<sub>2</sub> molecules in a cubic box of edge length 14.956 Å in the canonical (NVT) ensemble. Three-dimensional periodic boundary conditions were employed to obtain bulk behavior. The initial configuration of the system for the CPMD run was obtained from a well equilibrated run of classical MD using empirical potentials. The CPMD calculations were performed using density functional theory within the local density approximation (LDA) and employed Vanderbilt ultrasoft pseudopotentials.<sup>24</sup> The  $k=0$  point of the Brillouin zone was used in these simulations. A plane wave basis set with an energy cutoff of 25 Ry was found to be sufficient in obtaining converged energies and geometry for a CO<sub>2</sub> monomer, and was thus used for the bulk CPMD calculations as well. Given the rather large system size of 512 valence electrons, and a box edge of around 15 Å for the scCO<sub>2</sub> system, the choice of the ultrasoft pseudopotential is justified. Similar CPMD calculations have been successful in predicting properties of liquid water, methanol and a host of other molecular liquids.<sup>19,25</sup> The fictitious electronic mass was chosen to be 400 a.u. Its kinetic energy and that of the ions were controlled using Nosé–Hoover chain thermostats.<sup>26</sup> The equations of motion were integrated with a time step of 5 a.u. (around 0.12 fs) over a total run length of 12 ps (excluding an initial, equilibration time of 3 ps). The electronic degrees of freedom were quenched to the Born–Oppenheimer surface at the start of the CPMD run. The total energy was monitored during the entire CPMD trajectory, and was found to be conserved to 4 parts in 10<sup>6</sup>. Atomic configurations and velocities were stored every time step, which were later used for analyzing the structure and dynamics.

The classical MD simulations were performed using the EPM2 potential, which has been used earlier in simulations of liquid CO<sub>2</sub><sup>20</sup> as well as in studies of the water–CO<sub>2</sub> interface.<sup>27</sup> Here the C–O bond length was constrained to 1.149 Å, and a harmonic bending interaction for the intramolecular O–C–O angle was applied. Other details of the po-

tential were identical to those reported earlier.<sup>20</sup> These classical MD simulations were performed under NVT conditions for a system of 100 molecules in a cubic box with three-dimensional periodic boundary conditions. The MD equations of motion were integrated with a time step of 0.5 fs. Long range interactions were treated using the Ewald summation method. A distance cutoff of 10.7 Å was employed for truncating the nonbonded interactions.

Intermolecular partial structure factors were calculated using the following relation:

$$S_{\alpha\beta}(k) = \delta_{\alpha\beta} + 4\pi(\rho_{\alpha}\rho_{\beta})^{1/2} \int_0^{\infty} [g_{\alpha\beta} - 1] \frac{\sin kr}{kr} r^2 dr. \quad (1)$$

The total neutron weighted structure factor was obtained as<sup>28</sup>

$$S(k) = b_{\alpha}^2 S_{\alpha\alpha} + b_{\beta}^2 S_{\beta\beta} + 2b_{\alpha}b_{\beta} S_{\alpha\beta}, \quad (2)$$

where  $\rho_{\alpha} = N_{\alpha}/V$  is the number of atoms of the  $\alpha$ th component per unit volume and the neutron scattering lengths ( $b_{\alpha}$ ) for carbon and oxygen atoms are 6.646 and 5.805 fm, respectively.

## III. RESULTS AND DISCUSSION

### A. Molecular structure

In order to gain confidence in the use of this method with these approximations, we performed a calculation for optimization of the geometry of an isolated CO<sub>2</sub> molecule. Excellent agreement with the structure and vibrational spectrum reported experimentally was obtained. Specifically we obtained the C–O bond length to be 1.167 Å, and the O–C–O bond angle to be 180°, compared to the experimental value for the bond length of 1.162 Å.<sup>29</sup> CPMD calculations of the system containing 32 molecules in the supercritical state yielded an average C–O bond length of 1.169 Å. The intramolecular bond angle, averaged over the 32 molecules and over time was found to be 174.2° ± 0.4. This reduction in the bond angle relative to that for an isolated molecule, probably arises from intermolecular association as well as from thermal fluctuations. Such a deviation from perfect linearity can arise even if the O–O distance within a molecule is decreased by 0.01 Å from the value expected for a linear molecule. *Ab initio* calculations on charged CO<sub>2</sub> clusters,<sup>30</sup> and neutron diffraction experiments on supercritical carbon dioxide<sup>16</sup> have shown a similar marginal deviation from the linear geometry. Thus, the molecule in the supercritical state will possess a dipole moment. Unfortunately, we could not obtain an estimate of its magnitude due to the nature of the pseudopotential used in our simulations (calculation of the dipole moment for systems using the Vanderbilt ultrasoft pseudopotential has not been implemented yet in the CPMD program). However, preliminary calculations using the Troullier–Martins pseudopotential<sup>31</sup> for an isolated, bent CO<sub>2</sub> molecule with the average geometry reported here for the supercritical state (i.e., 1.169 Å and 174.2°) yields an estimate for the molecular dipole moment to be around 0.15 Debye.

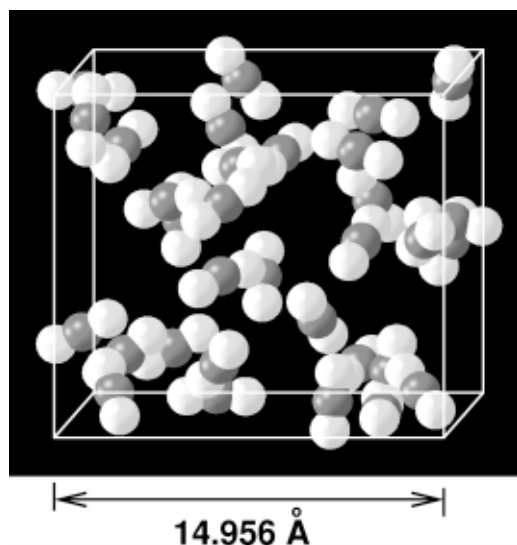


FIG. 1. Snapshot of a configuration of 32 molecules of  $\text{CO}_2$  in the supercritical state obtained from the CPMD simulations. Oxygen atoms are shown in white, and carbon atoms are in black.

## B. Near neighbor structure

A snapshot of the configuration of 32 molecules studied using CPMD is shown in Fig. 1. An observation of the total energy of the system during the course of the CPMD run did not indicate the disruption of any intramolecular C–O bond as expected at these state conditions. This is also borne out by the visualization presented in Fig. 1.

### 1. Pair correlation functions

We have studied the pair correlation function between the sites of different  $\text{CO}_2$  molecules in order to understand the structural features of this system. These are shown in Fig. 2 where a comparison is made between the results obtained from CPMD and from classical MD. The essential features of the pair correlation functions such as the position of the first peak, its minimum, the number of near neighbors, are summarized in Table I. Figure 2(a) displays  $g_{\text{CC}}(r)$ . The first neighbor C–C distance in the CPMD calculation is around 3.9 Å, as compared to a value of 4.3 Å from the MD calculation. The first peak in  $g_{\text{CC}}(r)$  of MD is shifted overall relative to the CPMD result. In addition, the first peak in this function for CPMD is marginally narrower than the corresponding MD result. Thus, the MD calculation overestimates to some extent the thickness of the first coordination shell. At the respective minima of the first peaks the coordination numbers are around 6.3 for the CPMD calculation, as compared to a value of around 9.5 for the MD run.

The intermolecular C–O pair correlation functions obtained from CPMD and MD are shown in Fig. 2(b). The CPMD distribution exhibits two well defined peaks one at 3.1 Å and the other at 4.1 Å. Although it is likely that these two peaks arise from the two oxygens of the same  $\text{CO}_2$  neighbor, a part of the contribution particularly to the second peak could come from  $\text{CO}_2$  neighbors who share only one oxygen atom within a distance of 5.7 Å [the first peak minimum in  $g_{\text{CO}}(r)$ ] from the carbon atom of the central molecule. In the following discussion, we denote the oxygen

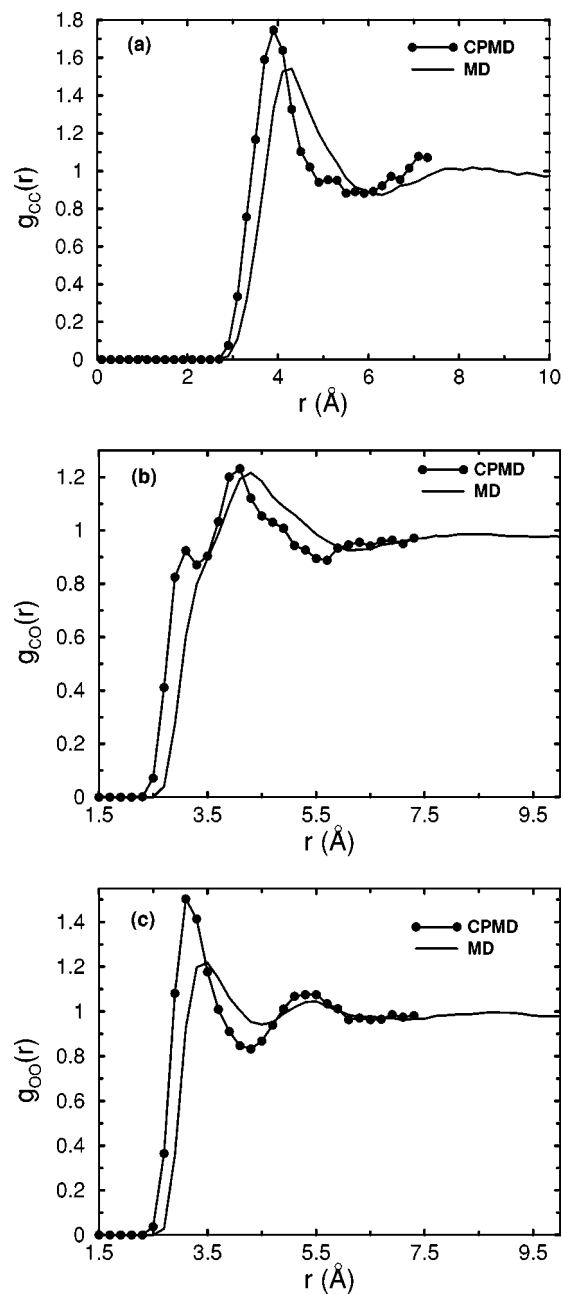


FIG. 2. Intermolecular radial distribution functions in supercritical  $\text{CO}_2$ . (a)  $g_{\text{CC}}(r)$ , (b)  $g_{\text{CO}}(r)$ , (c)  $g_{\text{OO}}(r)$ .

atom that falls within the first hump of  $g_{\text{CO}}(r)$  as  $\text{O}_a$ , and the one falling under the second hump as  $\text{O}_b$ . The number of oxygen neighbors at the first peak minimum of 3.3 Å is around 1.4. The nominal number of oxygen atoms at the minimum of the second hump (at 5.7 Å) is 13.8. Since the number of carbon neighbors [from  $g_{\text{CC}}(r)$ ] is 6.3, we can expect that twice the number of oxygens in the first coordination shell. The value of 13.8 obtained from  $g_{\text{CO}}(r)$  is reasonably close to this expectation, suggesting that the two humps in  $g_{\text{CO}}(r)$  probably arise from the same  $\text{CO}_2$  neighbor. The difference is likely to come from those neighbor molecules that do not have both their oxygen atoms within a distance of 6 Å of the carbon atom of the central  $\text{CO}_2$  molecule. The pair correlation function obtained from MD is

TABLE I. Summary of structural features.

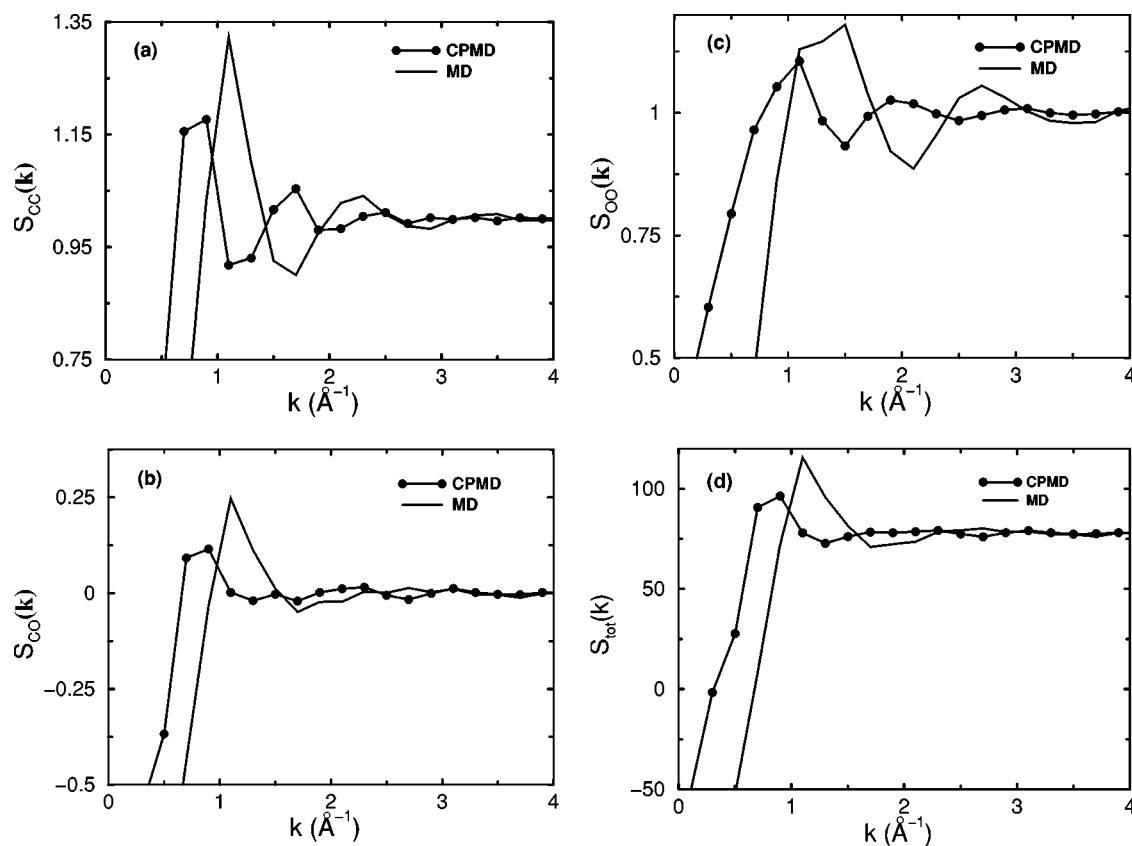
Quantity	$g_{CC}$		$g_{CO}$		$g_{OO}$	
	CPMD	MD	CPMD	MD	CPMD	MD
First peak (Å)	3.9	4.3	3.1, 4.1	4.3	3.1	3.5
First min (Å)	5.5	6.3	5.7	6.1	4.3	4.5
Coordination number	6.3	9.5	13.8	17.3	5.2	5.9

shifted to larger distances by about 0.2 Å relative to that from CPMD, quite similar to the observations in  $g_{CC}(r)$ . Also note that the prominent first hump (denoted as  $O_a$  above) present in the CPMD data of  $g_{CO}(r)$ , is absent in the classical MD result. In the absence of a clear hump in  $g_{CO}(r)$  obtained from the classical MD run,  $O_a$  for the MD results was defined through the change in slope of the pair correlation function that occurred at 3.2 Å. Although a hump or a peak is not clearly visible at this distance, an underlying feature at 3.2 Å is likely to be the cause for the change in slope. Hence one can suppose that the MD data agrees qualitatively with the CPMD result on the existence of a shorter near neighbor oxygen around a central carbon atom. The intermolecular  $g_{OO}(r)$  [Fig. 2(c)] obtained from CPMD exhibits a first peak at 3.1 Å, with a minimum at 4.3 Å. The coordination number at the minimum is around 5.2, in good agreement with the value expected from the preceding discussion on  $g_{CO}(r)$ . Again, we observe a marginal shift of about 0.4 Å in the function obtained from MD, relative to the result of CPMD.

The structure factors obtained from these pair correlation functions are shown in Fig. 3.

## 2. Angle distributions

As discussed in the Introduction, at higher densities of scCO<sub>2</sub>, near neighbor CO<sub>2</sub> molecules are possibly oriented in a distorted T-shaped geometry. Recently, Cipriani *et al.*<sup>21</sup> have predicted an arrangement in which the molecule in the first neighboring shell lies in the equatorial plane of the central molecule. We have examined this aspect by studying the distribution of the angle between molecular backbones of neighbors. We proceed by displaying a schematic of the near neighbor configuration in Fig. 4. Here,  $O_a$  is an oxygen atom that is within a distance of 3.1 Å from the carbon atom of the central CO<sub>2</sub> molecule.  $C_2$  is the carbon atom that is bonded to  $O_a$  and  $O_b$  is the second oxygen atom in this neighbor molecule. We show in Fig. 5, the distribution of angles made by the backbone vector (the  $OC_1$  vector) of the central molecule with the vectors,  $C_1O_a$ ,  $C_1C_2$ , and  $C_1O_b$ . In all the

FIG. 3. Partial structure factors and neutron weighted total structure factor of scCO<sub>2</sub>. (a)  $S_{CC}$ , (b)  $S_{CO}$ , (c)  $S_{OO}$ , (d)  $S_{tot}$ .



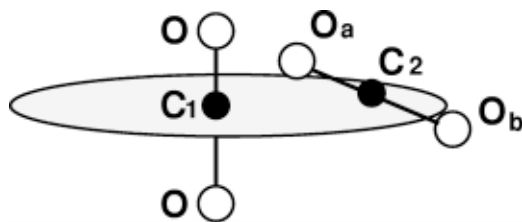


FIG. 4. Schematic of the arrangement of near neighbor molecules in  $sc\text{CO}_2$ .  $O_a$  is the oxygen atom of the neighboring molecule that is closest to the carbon atom ( $C_1$ ) of the central molecule.

three cases, a preference for perpendicular orientation is observed. However, the  $\text{OC}_1\text{C}_2$  and the  $\text{OC}_1\text{O}_b$  distributions are relatively flatter as compared to the distribution of  $\text{OC}_1\text{O}_a$  angles. Thus, our data indicates that although a

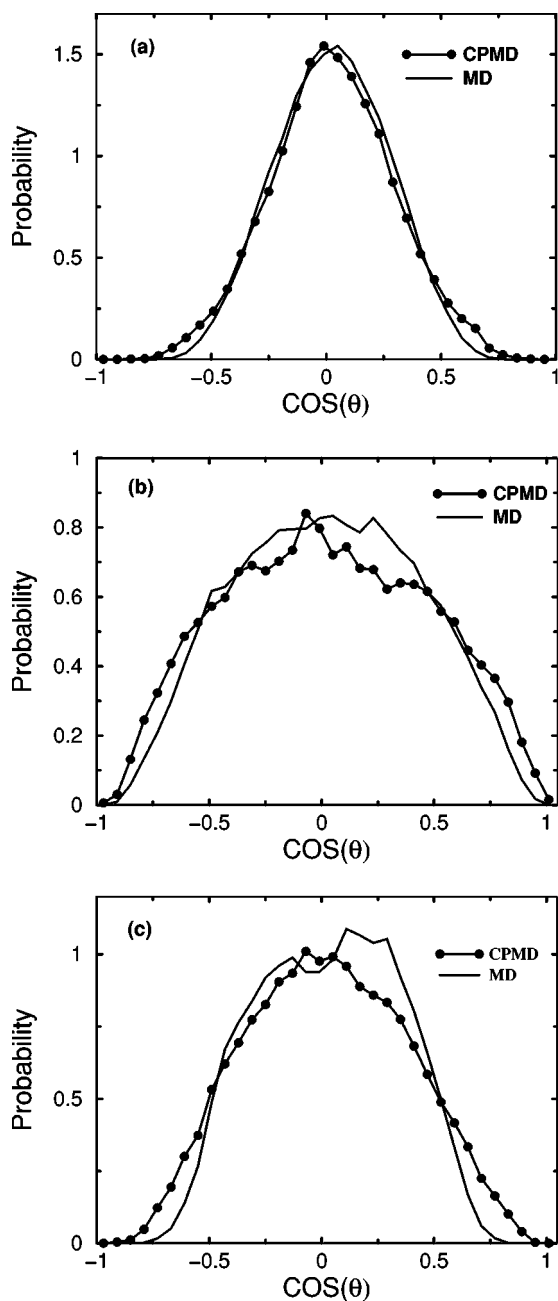


FIG. 5. Angular distribution of molecules in the first coordination shell. (a)  $\text{OC}_1\text{O}_a$ , (b)  $\text{OC}_1\text{O}_b$ , (c)  $\text{OC}_1\text{C}_2$ .

T-shaped near neighbor configuration is preferred, a significant fraction of neighbors could be oriented such that the  $O_a$  atom of the neighbor and its carbon ( $C_2$ ) are in the equatorial plane of the central  $\text{CO}_2$  molecule, while the  $O_b$  atom exhibits a tendency to be out of this plane.

However, when a near neighbor condition based on the C–C distance is imposed [based on the minimum of the first peak of the  $g_{\text{CC}}(r)$ , i.e., 5.7 Å], the distribution of  $\text{OCC}$  angles shows no preference (not shown). One obtains a featureless distribution that indicates an isotropic distribution of carbon atoms around the central molecule. We believe that these results are not inconsistent with each other; rather they indicate that molecules in the closest shell (as defined by the C–O distance cutoff) exhibit orientational preferences which die rather quickly as one increases the shell envelope. It should also be noted that this closest shell is not defined well as the minimum of the first peak in the  $g_{\text{CO}}(r)$  has a value of around 0.88. This result explains the loss in orientational preferences of near neighbors with increasing distance.

## C. Dynamics

### 1. Reorientational dynamics

The timescales of reorientation of a  $\text{CO}_2$  molecule in  $sc\text{CO}_2$  are crucial to understanding its ability to solvate other species. We examine this quantity through the time correlation function of the vector  $\mathbf{R}$ ,<sup>32</sup> that connects the two oxygen atoms of the molecule, as

$$C_\ell^r(t) = \frac{\langle P_\ell(\mathbf{R}_i(0) \cdot \mathbf{R}_i(t)) \rangle}{\langle P_\ell(\mathbf{R}(0) \cdot \mathbf{R}(0)) \rangle}, \quad (3)$$

where the angular brackets denote averaging over molecular index  $i$ , and over the initial time value 0.  $P_\ell$  is the Legendre polynomial of order  $\ell$ . The time correlation function (TCF) for  $\ell=1$  is related to the infrared spectrum and that for  $\ell=2$  relates to the depolarized Raman spectrum of the system. We show the TCFs for  $\ell=1$  and  $\ell=2$ , for the systems simulated using CPMD and using MD in Fig. 6.

The TCF obtained from CPMD, for  $\ell=1$  exhibits a plateau region between 1 ps and about 2 ps, after an initial fast decay, which is absent in the function obtained from MD. The average time constants of this relaxation can be obtained by integration of these functions over time, as

$$\tau_{\ell,r} = \int_0^\infty C_\ell^r(t) dt. \quad (4)$$

These values obtained from MD and CPMD are compared in Table II. The CPMD result for  $\tau_{2,r}$  of 268 fs is in close agreement with the value of 250 fs obtained by  $^{17}\text{O}$  relaxation rate ( $1/T_1$ ) measurements by Holz *et al.*,<sup>33</sup> of Umecky *et al.*,<sup>34</sup> and the classical MD results of Adams and Siavosh-Haghighi.<sup>35</sup> The time constants obtained from MD for both the functions are smaller than that obtained from the CPMD simulations. Although the TCFs are quite close to each other for times less than 500 fs, they tend to differ at longer times. The initial decay is likely to arise from inertial rotation and classical MD captures it well, while at the intermediate time scales of 1 to 2 ps, it decays faster than the

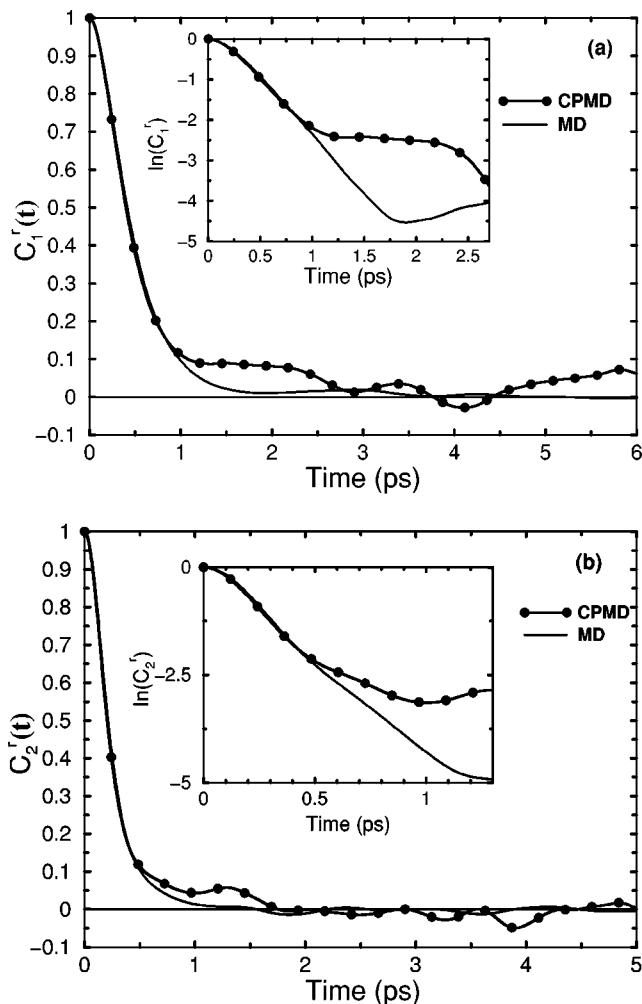


FIG. 6. Reorientational time correlation functions,  $C_l^r(t)$ , of CO<sub>2</sub> for (a)  $l=1$ , and (b)  $l=2$ . Insets show the short-time decay in logarithmic scale.

CPMD result. The entire length of the CPMD and of the MD analysis trajectories (12 and 20 ps, respectively) were employed for these calculations. These run lengths are longer than the relaxation times of the TCFs. Thus it is unlikely that the difference between the CPMD and the MD result arises from the shorter run length of the former.

TABLE II. Dynamical properties of scCO<sub>2</sub>.

Quantity	CPMD	MD	Experiment
$\tau_{1r}$ (fs)	620	520	...
$\tau_{2r}$ (fs)	268	246	250 <sup>a</sup>
D ( $10^{-4} \times \text{cm}^2/\text{s}$ )	2.29 (MSD) 2.50 (VACF)	2.17 (MSD) 2.62 (VACF)	2.02 <sup>b</sup>
Vibrational frequencies ( $\text{cm}^{-1}$ )	1228 ( $\nu_1$ )		1281 <sup>c</sup> ( $\nu_1$ )
	1319 ( $\nu_1$ )	...	1387 <sup>c</sup> ( $\nu_1$ )
	628 ( $\nu_2$ )	...	667 <sup>d</sup> ( $\nu_2$ )
	697 ( $\nu_2$ )	...	
	2309 ( $\nu_3$ )		2318 <sup>e</sup> ( $\nu_3$ )

<sup>a</sup>Estimate from Ref. 33.

<sup>b</sup>Reference 36.

<sup>c</sup>References 40 and 41.

<sup>d</sup>For isolated CO<sub>2</sub> molecule.

<sup>e</sup>Estimate from Refs. 37 and 38.

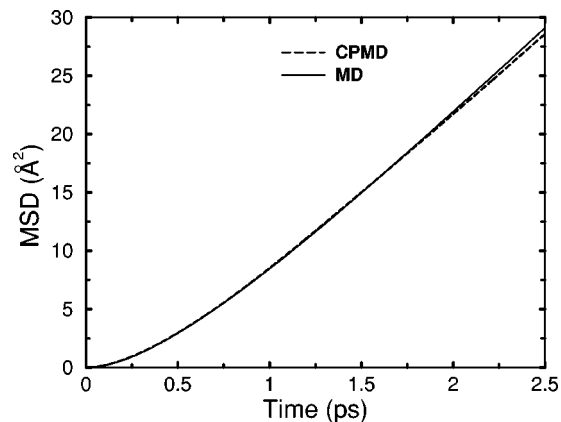


FIG. 7. Mean-square displacement of CO<sub>2</sub> molecules in supercritical state.

## 2. Translational dynamics

We characterize the translational motion of the CO<sub>2</sub> molecules in the two simulations by the usual quantity, i.e., by their mean-squared displacement (MSD). We compare these results in Fig. 7. First, although the time scales of investigation are small (few picoseconds), the values of displacements are healthy as the system is in the supercritical state. Experience in MD simulations have taught us that the MSD data can exhibit quite different slopes for different blocks of the MD trajectory in a generic liquid. However, in this case since the values of MSD are large, it is possible to trust the data obtained from limited run lengths. The functions for CPMD and for MD are nearly identical. The diffusion coefficient obtained from CPMD calculations is found to be  $2.29 \times 10^{-4} \text{ cm}^2/\text{s}$ , while that from MD is  $2.17 \times 10^{-4} \text{ cm}^2/\text{s}$ . The results are in good agreement with the value of  $2.02 \times 10^{-4} \text{ cm}^2/\text{s}$ , obtained from the <sup>17</sup>O NMR spin-lattice relaxation time measurements.<sup>36</sup>

## 3. Velocity correlations and vibrational spectrum

The normalized velocity auto time correlation functions of carbon and oxygen atoms are shown in Fig. 8. The integral of the unnormalized function for carbon atoms is related to the diffusion coefficient of the molecule. The value calculated thus from the CPMD run, is found to be  $2.50 \times 10^{-4}$

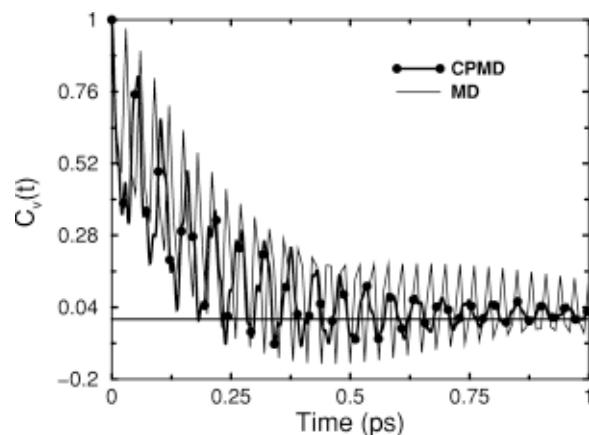


FIG. 8. Normalized velocity autocorrelation functions obtained from CPMD and MD simulations.

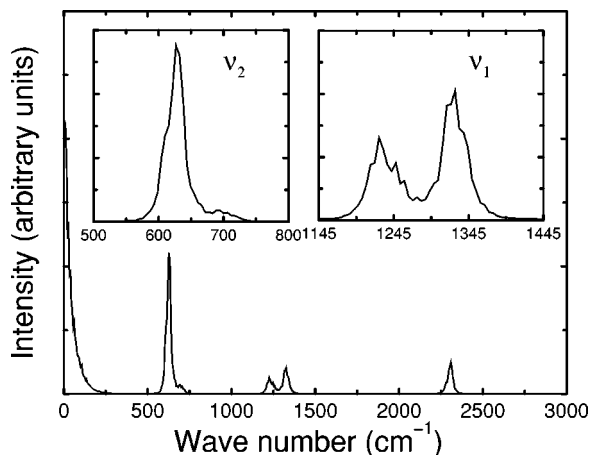


FIG. 9. Vibrational spectrum of supercritical  $\text{CO}_2$  obtained as the Fourier transform of velocity autocorrelation function from the CPMD calculation. The region around the symmetric stretch mode ( $\nu_1$ ) and the bending mode ( $\nu_2$ ) are shown in an expanded scale in the inset.

$\text{cm}^2/\text{s}$  and compares well with the estimate obtained from the MSD data that used the Einstein relation. These velocity correlation functions can be Fourier transformed to obtain the power spectrum or the vibrational density of states (VDOS). We show this data in Fig. 9. Three distinct features are evident; the asymmetric stretch frequency ( $\nu_3$ ) is observed at  $2309 \text{ cm}^{-1}$ , in comparison to the experimental value of  $2318 \text{ cm}^{-1}$  for  $\text{scCO}_2$  (estimated from Refs. 37 and 38), and a value of  $2349 \text{ cm}^{-1}$  for the isolated  $\text{CO}_2$  molecule. The bending mode ( $\nu_2$ ) is twofold degenerate and is observed at  $667 \text{ cm}^{-1}$  for the case of an isolated, linear  $\text{CO}_2$  molecule. In the CPMD calculations of  $\text{scCO}_2$ , we observe a large peak at  $628 \text{ cm}^{-1}$  and a small hump at  $697 \text{ cm}^{-1}$ . As noted earlier, the geometry of the molecule is nonlinear. It is possible that this additional feature at  $697 \text{ cm}^{-1}$  could come from this deformation. Such a splitting of the bending mode has earlier been observed for  $\text{CO}_2$  sequestered in poly(methyl methacrylate) films and has been ascribed to the interaction between the electron lone pairs of the carbonyl oxygen (of the polymer) with the carbon atom of the  $\text{CO}_2$  molecule.<sup>39</sup> We believe that the distorted T-shaped geometry of near neighbor molecules in  $\text{scCO}_2$  lifts the degeneracy of the bending mode in a similar fashion. The symmetric stretch ( $\nu_1$ ) in isolated  $\text{CO}_2$  is infrared inactive but is Raman active. Usually, this mode is observed as a split peak, the splitting arising from the combination of the fundamental of the symmetric stretch mode and the first overtone of the bending mode, a process called the Fermi resonance. The CPMD vibrational spectrum shows two peaks in this region, one at  $1228 \text{ cm}^{-1}$ , and the other at  $1319 \text{ cm}^{-1}$ , probably arising from the same combination. Experimentally, these are observed at  $1281$  and  $1387 \text{ cm}^{-1}$ , respectively, in the supercritical state<sup>40,41</sup> and at  $1388 \text{ cm}^{-1}$  for the isolated molecule. It is important to note that all the vibrational features observed for  $\text{scCO}_2$  through the CPMD calculations, show a red shift in the peak frequencies relative to the experimental data for an isolated  $\text{CO}_2$  molecule, the shift arising out of intermolecular interactions. Such a red shift is observed in the experimental vibrational spectrum of  $\text{scCO}_2$  as well,<sup>38</sup> although to a lesser extent than

what is observed in these CPMD calculations. The differences between experiments and the current simulations could also be due to the local density approximation employed in our study. At zero frequency, the VDOS obtained from CPMD has a nonzero value, due to the presence of rigid body translational and rotational modes in the system.

#### IV. CONCLUSIONS

We have performed *ab initio* MD calculations of supercritical carbon dioxide and have compared these results with experiments and against conventional MD simulations that employ empirical potentials. Expectedly, CPMD calculations agree quite well with experiments both in terms of the structure, and in dynamics. These CPMD calculations could form a baseline for future analyses and comparisons to both theory and to experiment.

The ability of  $\text{scCO}_2$ , despite its low density, and its supposed lack of a molecular dipole moment, to solvate a wide variety of substances has long been a puzzle. Our calculations reveal that (a) the  $\text{CO}_2$  molecule possesses a dipole moment, however small, that arises out of a change in the internal geometry of the molecule due to a polarization of charge density from intermolecular interactions, and (b) a reasonably ordered near neighbor molecular structure exists at the state point studied here. The combination of these two observations along with the molecular quadrupole moment may partially explain the capacity of  $\text{scCO}_2$  to solvate other species. Isolated  $\text{CO}_2$  has a quadrupole moment of  $4.1 \times 10^{-26} \text{ esu}$ .<sup>42</sup> As remarked earlier, the presence of T-shaped near neighbor configurations has been attributed to the nonzero quadrupole moment.<sup>21</sup> The relative strengths of the dipole and quadrupole moments in mediating  $\text{scCO}_2$ -solute interactions needs to be studied further.

We observe a well defined near neighbor structure in the supercritical state. The pair correlation function of intermolecular C–O pairs, exhibits two clear peaks which enabled us to study in detail, the arrangement of molecules around a central  $\text{CO}_2$ . We find the molecules in the first coordination shell to be arranged in a distorted T-shaped geometry. Although intermolecular distances were found to be marginally larger in the MD calculations, the intermolecular angle distributions from MD were found to be in good agreement with CPMD data. The reorientational dynamics of  $\text{CO}_2$  plays an important role in its ability to solvate other species. In this respect, the CPMD calculations were found to match very well the rotational time scales obtained from NMR experiments. The rotational time constants for relaxation of the first-order and the second-order reorientational TCFs were found to be  $620$  and  $268 \text{ fs}$ , respectively. The MD results for the same agreed with the CPMD data for timescales less than a picosecond, but they do not reproduce the plateau found in the CPMD results between  $1$  and  $2 \text{ ps}$ . Hence the time constants obtained from MD calculations were, smaller than that obtained from CPMD. The vibrational density of states obtained from the velocity auto correlation functions of the atoms reproduced the key observations of experiments—a red shift in the frequencies of the modes relative to that for

an isolated molecule was observed, and the splitting of the symmetric stretch peak due to Fermi resonance was reproduced in the CPMD calculations. Needless to state, the MD calculations involving no internal degrees of freedom cannot be expected to capture the vibrational modes of the molecules in scCO<sub>2</sub>.

The results of the present CPMD simulations could be used to refine the interaction parameters of carbon dioxide for use in classical MD simulations. Specifically, the relevance of retaining the linear structure of the molecule in the supercritical state in such simulations, could be examined. In an interesting study on the vibrational relaxation of I<sub>2</sub><sup>-</sup> ions in carbon dioxide clusters, Ladanyi and Parson<sup>43</sup> have observed a spontaneous solvent polarization for an artificially constructed hyperflexible solvent model. Our results on the possibility of the existence of a permanent dipole moment for carbon dioxide molecules in the supercritical state are relevant to such studies. The marginal differences observed between the CPMD and the MD calculations could also arise from system size effects.<sup>18</sup> Our CPMD calculations involve only 32 molecules—this could influence the results, by artificially suppressing density heterogeneities of length scales larger than 7.5 Å, which is around half of the simulation box length used in the CPMD study. However, we wish to point out that a box of about 15 Å itself is quite large by CPMD standards, and tremendous resources are required to study systems of larger sizes. We had performed MD calculations at two system sizes, one with 32 molecules and the other with 100 molecules and found the structural and dynamical data not to be too dependent on the size of the system. This makes us believe that the CPMD calculations involving 32 molecules are likely to be converged with respect to the size of the system and thus to be realistic of bulk behavior.

Dispersive forces have long been an issue in density-functional theory (DFT), and efforts have been made recently to treat van der Waals interactions more accurately.<sup>44,45</sup> In light of this, the excellent agreement obtained by our CPMD simulations with experiments could be due to a fortuitous cancellation of minor errors, or could point to the dominance of electrostatic interactions in supercritical carbon dioxide. This needs to be studied further. One needs to also compare the results obtained within the local density approximation with that obtained using a functional that includes gradient corrections. The former has been shown to underestimate intermolecular bond lengths.<sup>25</sup> High pressure solid phases of carbon dioxide have been studied using gradient corrected functionals,<sup>46</sup> and their use in predicting the properties of scCO<sub>2</sub> could be explored. Another aspect that requires detailed analyses is the electronic structure of this system. This would play a significant role in our understanding of the nature of interactions involved in solvation of solutes in scCO<sub>2</sub>.<sup>47</sup> This too shall be the object of future studies.

## ACKNOWLEDGMENTS

We thank the Center for Development of Advanced Computing, Bangalore, for a generous time allocation on

their Central Terascale Supercomputing Facility where these calculations were performed. We acknowledge helpful discussions with M. Krishnan.

- <sup>1</sup>M. Poliakoff and P. King, *Nature (London)* **412**, 125 (2001).
- <sup>2</sup>J. M. DeSimone, *Science* **297**, 799 (2002).
- <sup>3</sup>W. Leitner, *Nature (London)* **405**, 129 (2000).
- <sup>4</sup>S. L. Wells and J. DeSimone, *Angew. Chem., Int. Ed. Engl.* **40**, 518 (2001).
- <sup>5</sup>M. J. Clarke, K. L. Harrison, K. P. Johnston, and S. M. Howdle, *J. Am. Chem. Soc.* **119**, 6399 (1997).
- <sup>6</sup>W. Leitner, *Acc. Chem. Res.* **35**, 746 (2002); W. Leitner, *C.R. Acad. Sci. Paris* **3**, 595 (2000).
- <sup>7</sup>D. J. Heldebrant and P. G. Jessop, *J. Am. Chem. Soc.* **125**, 5600 (2003).
- <sup>8</sup>J. M. DeSimone, Z. Guan, and C. S. Elsbernd, *Science* **257**, 945 (1992).
- <sup>9</sup>M. J. Clarke, K. L. Harrison, K. P. Johnston, and S. M. Howdle, *J. Am. Chem. Soc.* **1997**, 119.
- <sup>10</sup>K. Nagashima, C. T. Lee, Jr., B. Xu, K. P. Johnston, J. M. DeSimone, and C. S. Johnson, Jr., *J. Phys. Chem. B* **107**, 1962 (2003).
- <sup>11</sup>B. Chen, J. I. Siepmann, and M. L. Klein, *J. Phys. Chem. B* **105**, 9840 (2001).
- <sup>12</sup>S. Salaniwal, S. T. Cui, P. T. Cummings, and H. D. Cochran, *Langmuir* **15**, 5188 (1999); S. Salaniwal, S. T. Cui, H. D. Cochran, and P. T. Cummings, *ibid.* **17**, 1773 (2001).
- <sup>13</sup>S. Senapati, J. S. Keiper, J. M. DeSimone, G. D. Wignall, Y. B. Melnichenko, H. Frielinghaus, and M. L. Berkowitz, *Langmuir* **18**, 7371 (2002).
- <sup>14</sup>P. Cipriani, M. Nardone, and F. P. Ricci, *Physica B* **241–243**, 940 (1998); S. Chiappini, M. Nardone, and F. P. Ricci, *Mol. Phys.* **89**, 975 (1996).
- <sup>15</sup>K. Nishikawa and M. Takematsu, *Chem. Phys. Lett.* **226**, 359 (1994); T. Morita, K. Nishikawa, M. Takematsu, H. Iida, and S. Furutaka, *J. Phys. Chem. B* **101**, 7158 (1997).
- <sup>16</sup>R. Ishii, S. Okazaki, O. Odawara, I. Okada, M. Misawa, and T. Fukunaga, *Fluid Phase Equilib.* **104**, 291 (1995); R. Ishii, S. Okazaki, I. Okada, M. Furusaka, N. Watanabe, M. Misawa, and T. Fukunaga, *J. Chem. Phys.* **105**, 7011 (1996).
- <sup>17</sup>G. Tabacchi, C. J. Mundy, J. Hutter, and M. Parrinello, *J. Chem. Phys.* **117**, 1416 (2002).
- <sup>18</sup>S. C. Tucker, *Chem. Rev.* **99**, 391 (1999).
- <sup>19</sup>J. A. Morrone and M. E. Tuckerman, *J. Chem. Phys.* **117**, 4403 (2002).
- <sup>20</sup>J. G. Harris and K. H. Yung, *J. Phys. Chem.* **99**, 12021 (1995).
- <sup>21</sup>P. Cipriani, M. Nardone, F. P. Ricci, and M. A. Ricci, *Mol. Phys.* **99**, 301 (2001).
- <sup>22</sup>S. Okazaki *et al.*, *J. Chem. Phys.* **105(16)**, 7011 (1996).
- <sup>23</sup>J. Hutter, P. Ballone, M. Bernasconi, P. Focher, E. Fois, S. Goedecker, D. Marx, M. Parrinello, and M. E. Tuckerman, CPMD Version 3.07.2, Max Planck Institut fuer Festkoerperforschung, Stuttgart, and IBM Zurich Research Laboratory, 1990–2003.
- <sup>24</sup>D. Vanderbilt, *Phys. Rev. B* **41**, 7892 (1990).
- <sup>25</sup>K. Laasonen, M. Sprik, M. Parrinello, and R. Car, *J. Chem. Phys.* **99**, 9080 (1993); K. Laasonen and M. L. Klein, *J. Am. Chem. Soc.* **116**, 11620 (1994); A. J. Sillanpaa, C. Simon, M. L. Klein, and K. Laasonen, *J. Phys. Chem. B* **106**, 11315 (2002).
- <sup>26</sup>G. J. Martyna, M. E. Tuckerman, and M. L. Klein, *J. Chem. Phys.* **97**, 2635 (1992).
- <sup>27</sup>S. R. P. Rocha, K. P. Johnston, R. E. Westacott, and P. J. Rossky, *J. Phys. Chem. B* **105**, 12092 (2001).
- <sup>28</sup>N. H. March and M. P. Tosi, *Atomic Dynamics in Liquids* (Dover, New York, 1991).
- <sup>29</sup>G. Herzberg, *Electronic Spectra and Electronic Structure of Polyatomic Molecules* (Van Nostrand, New York, 1966).
- <sup>30</sup>I. A. Shkrob, *J. Phys. Chem. A* **106**, 11871 (2002).
- <sup>31</sup>N. Troullier and J. L. Martins, *Phys. Rev. B* **43**, 1993 (1991).
- <sup>32</sup>A. S. Haghghi and J. E. Adams, *J. Phys. Chem. A* **105**, 2680 (2001).
- <sup>33</sup>M. Holz, R. Haselmeier, A. J. Dyson, and H. Huber, *Phys. Chem. Chem. Phys.* **2**, 1717 (2000).
- <sup>34</sup>T. Umecky, M. Kanakubo, and Y. Ikushima, *J. Phys. Chem. B* **107**, 12003 (2003).
- <sup>35</sup>J. E. Adams and A. S. Haghghi, *J. Phys. Chem. B* **106**, 7973 (2001).
- <sup>36</sup>P. Etesse, J. A. Zega, and R. Kobayashi, *J. Chem. Phys.* **97**, 2022 (1992).
- <sup>37</sup>C. Yokoyama, Y. Kanno, M. Takahashi, K. Ohtake, and S. Takahashi, *Rev. Sci. Instrum.* **64**, 1369 (1993).
- <sup>38</sup>J. P. Blizt, C. R. Yonker, and R. D. Smith, *J. Phys. Chem.* **93**, 6661 (1989).



- <sup>39</sup>S. G. Kazarian, M. F. Vincent, F. V. Bright, C. L. Liotta, and C. A. Eckert, *J. Am. Chem. Soc.* **118**, 1729 (1996).
- <sup>40</sup>Y. Yagi, H. Tsugane, H. Inomata, and S. Saito, *J. Supercrit. Fluids* **6**, 139 (1993).
- <sup>41</sup>M. Poliakoff, S. M. Howdle, and S. G. Kazarian, *Angew. Chem., Int. Ed. Engl.* **34**, 1275 (1995).
- <sup>42</sup>A. D. Buckingham and R. L. Disch, *Proc. R. Soc. London, Ser. A* **273**, 275 (1963).
- <sup>43</sup>B. M. Ladanyi and R. Parson, *J. Chem. Phys.* **107**, 9326 (1997).
- <sup>44</sup>W. Kohn, Y. Meir, and D. E. Makarov, *Phys. Rev. Lett.* **80**, 4153 (1998).
- <sup>45</sup>M. Kamiya, T. Tsuneda, and K. Hirao, *J. Chem. Phys.* **117**, 6010 (2002).
- <sup>46</sup>S. A. Bonev, F. Gygi, T. Ogitsu, and G. Galli, *Phys. Rev. Lett.* **91**, 065501 (2003).
- <sup>47</sup>J. F. Kauffman, *J. Phys. Chem. A* **105**, 3433 (2001).